



Topological Fluid Dynamics II

# Estimating topological entropy from the motion of stirring rods

Sarah E. Tumas and Jean-Luc Thiffeault\*

*Department of Mathematics, University of Wisconsin – Madison, 480 Lincoln Drive, Madison, WI, 53706, USA*

## Abstract

Stirring a two-dimensional viscous fluid with rods is often an effective way to mix. The topological features of periodic rod motions give a lower bound on the topological entropy of the induced flow map, since material lines must ‘catch’ on the rods. But how good is this lower bound? We present examples from numerical simulations and speculate on what affects the ‘gap’ between the lower bound and the measured topological entropy. The key is the sign of the rod motion’s action on first homology of the orientation double cover of the punctured disk.

© 2012 Published by Elsevier Ltd. Selection and/or peer-review under responsibility of K. Bajer, Y. Kimura, & H.K. Moffatt.

**Keywords:** fluid stirring ; topological entropy ; braids

## 1. Introduction

The paper of Boyland, Aref & Stremler [1] pioneered the study of two-dimensional rod-stirring devices using tools from topological surface dynamics. The central idea is that some rod motions impose a minimal complexity to the fluid trajectories, resulting in good mixing in at least part of the domain. Since then, many studies have followed: these include several papers dealing directly with rod motion [2, 3, 4, 5, 6, 7, 8, 9, 10]; various work on vortices, ‘ghost rods,’ and almost-invariant sets [11, 12, 13, 14, 15, 16, 17]; papers on the topology of chaotic trajectories and random braids [18, 19, 20, 21, 22, 23, 24]; a paper on an extension to three dimensions using stationary rod inserts [25]; and a review [26] and magazine article [27].

Throughout all this, there remains a vexing question, first raised by Phil Boyland: if one studies the rod motion depicted in Fig. 1(a), which is denoted  $\sigma_1\sigma_2^{-1}$  in terms of braid group generators, the growth rate of material lines *in the fluid* is almost the same as that predicted by the rod motion, which is a lower bound. How do we explain such a small discrepancy (or gap) between the lower bound and the measured value? Here we do not propose a full solution to this problem, but instead offer some observations, based on numerical simulations, of when the lower bound is and isn’t sharp, what this correlates with, and speculate on possible causes. At the heart of the matter is ‘secondary folding,’ or the observation that in some cases material lines fold a lot more than is strictly required by the topology

\* Corresponding author. Tel.: +1-608-263-4089 ; fax: +1-608-263-8891 .  
E-mail address: [jeanluc@math.wisc.edu](mailto:jeanluc@math.wisc.edu)

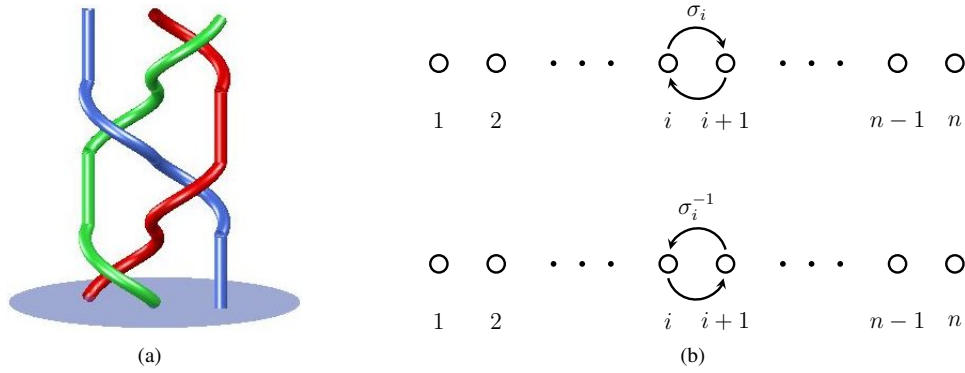


Fig. 1. (a) Motion of rods in a 3-rod mixer described by the braid  $\sigma_1 \sigma_2^{-1}$ . The vertical axis is time, and two full periods are shown. (b) The braid generator  $\sigma_i$  (top) is a clockwise interchange of the  $i$ th and  $(i+1)$ th rods, with all other rods held fixed. Its inverse,  $\sigma_i^{-1}$  (bottom), is a counter-clockwise interchange of the same two rods.

of the rod motion. This issue was explored in detail by the authors for toral linked twist maps [28, 29]. Here we focus on physical rod-stirring devices, also called rod mixers.

We can also interpret a small gap in terms of ‘taffy pullers’ [10]. Ignore the fluid and consider a plastic ‘strap’ wrapped around the rods. As the rods move, imagine the plastic strap can stretch, but can never shrink. The motions with a small gap described below will lead to a plastic strap that never develops any slack throughout the entire rod motion. The question is to determine what properties of a braid are needed to ensure this.

## 2. Braid-based rod mixers

We consider rod-stirring devices or mixers that are constructed such that the rod motion is described by *braids* [30, 31, 32]. In these two-dimensional circular containers, the rods start along a fixed horizontal line and move in accordance with *braid generators*,  $\sigma_i^{\pm 1}$ , depicted in Figure 1(b). For example, in a 3-rod mixer given by the braid  $\sigma_1 \sigma_2^{-1}$  [1], first the two leftmost rods move halfway around a circle in a clockwise direction clockwise. Immediately after that, the two rightmost rods move halfway around a circle in a counter-clockwise direction (Figure 1(a)). The circular paths are centred directly between the two rods, and have diameter equal to the rod spacing. The speed of the rods is immaterial, since we are only considering Stokes (slow viscous) flow.

More generally, we write the stirring motion for  $n$  rods as a braid expressed as a sequence of generators,  $\sigma_i$ ,  $i = 1, \dots, n-1$ . Each generator represents the clockwise interchange of the  $i$ th and  $(i+1)$ th strands or rods. The inverse,  $\sigma_i^{-1}$ , is a counter-clockwise interchange (Figure 1(b)). Note that the strands are always numbered from left to right, so a given subscript does not always refer to the same rod. By having the rods move in the same way as a specific braid, we can directly and systematically compare the measured topological entropy in the fluid system to the lower bound predicted by the braid (via the isotopy class [33, 34, 35]).

*Remark.* There are different conventions in the literature: In some papers  $\sigma_i$  is defined as the counter-clockwise interchange, which is the opposite of our definition. There are also differing conventions on composition order. We will always write generators from left to right – that is, in the braid  $\sigma_1 \sigma_2$ , the  $\sigma_1$  interchange occurs *before* the  $\sigma_2$  interchange.

*Remark.* The lower bound on the entropy, based on the braid, is independent of the specific details of the rod motion. However, the measured flow entropy depends in general on the rod radius, rotation, and how near the rods come to each other and to the outer wall of the container during their motion. In our simulations, the rod radii are relatively small and we keep them from coming too close to the wall to avoid extra growth of material lines due to image effects. Our simulations were performed with the computer program *Flop*, by Matthew D. Finn, Emmanuelle Gouillart, and

J.-L.T. The program is based on the complex-variable method described in [2]. We measure the flow topological entropy  $h$  from the growth rate of material lines in the flow [36, 37, 38].

### 2.1. Three-rod mixers

We start by looking at devices with three rods. In particular, we will focus on motions based on braids of the form  $\sigma_1^k \sigma_2^{-\ell}$ . When  $k\ell > 0$ , we call the braid *counter-rotating*; when  $k\ell < 0$  we call it *co-rotating*. Braids of this form are *pseudo-Anosov* if and only if  $|2 + k\ell| > 2$ . All counter-rotating braids are pseudo-Anosov, but co-rotating braids are only pseudo-Anosov if  $k\ell < -4$ . Braids that are not pseudo-Anosov are *finite order* or *reducible*, according to the Thurston–Nielsen classification theorem [33, 34, 35]. We will not encounter any reducible braids in this paper.

Figure 2 shows an iterated material line for several different braid mixers. The three in the left column are counter-rotating, and the three in the right column are co-rotating. Of the six braid mixers shown in Figure 2, five are pseudo-Anosov and one is not. With only a quick glance, it is not hard to guess that  $\sigma_1 \sigma_2$  is the odd one out – in comparison to the others, the material line in that device has hardly stretched at all, even after 9 periods, and pseudo-Anosov braids have an exponential line stretching rate [33, 34, 35].

However, despite the fact that the braid  $\sigma_1 \sigma_2$  is not pseudo-Anosov, we still measure a positive topological entropy for the *flow* in the mixing device. In fact, the braid mixers tend to fall into two categories: those where the flow entropy  $h$  is close to the braid entropy  $h_{\text{rods}}$  (of the order of 10% difference), and those where  $h$  is considerably larger than  $h_{\text{rods}}$  (> 25% difference). Table 1 shows, for several braids of the form  $\sigma_1^k \sigma_2^{-\ell}$ , the measured topological entropy in the braid mixer ( $h$ ) and the lower bound obtained from the rod braid ( $h_{\text{rods}}$ ). The last column gives the ‘gap’ between the two values, expressed as a percentage of  $h$ . The first set of braids is counter-rotating ( $k\ell < 0$ ); the second set co-rotating ( $k\ell > 0$ ). Note that the counter-rotating mixers show a small gap, and the co-rotating ones have a much larger gap.

The penultimate column of Table 1 gives the sign of the dominant eigenvalue (the one with the largest magnitude) of the Burau matrix representation of the braid. The Burau representation [39, 31, 40, 41, 42] arises from an action of the braid on first homology of a double cover of the punctured disk (actually a  $\mathbb{Z}$ -cover, but we only use the double cover here). Figure 3 depicts the construction of the double cover for a disk with three rods. Notice in Table 1 that for the pseudo-Anosov braids ( $h_{\text{rods}} > 0$ ), all the counter-rotating cases have a negative Burau eigenvalue, while all the co-rotating cases have a positive eigenvalue. For the non-pseudo-Anosov braids (i.e. those of finite order), the eigenvalue of the Burau matrix is always on the unit circle (complex), so we do not record a sign.

For 3-braids, the logarithm of the spectral radius of the Burau matrix agrees with the topological entropy of the braid. For pseudo-Anosov braids this largest eigenvalue is real but can be either positive or negative. A negative eigenvalue corresponds to a ‘flip’ of the homological generators at every application of the braid. For toral linked twist maps, this is associated with ‘kinks’ in the material lines, as shown in [28]. These are what we call ‘secondary folds,’ as depicted for a fluid system in Figure 5 and discussed in Section 3.1). The conjecture is that these kinks lead to additional growth of material lines, thus causing extra entropy above the lower bound. However, this connection has not been yet rigorously demonstrated.

### 2.2. Four-rod mixers

We now look at four-rod mixing devices. With four rods, there is no sense in classifying braids as counter- or co-rotating. Instead, we will focus on the sign of the dominant eigenvalue of the Burau matrix. Since we have more than three rods, the dominant eigenvalue of the Burau matrix is no longer guaranteed to give the topological entropy of the braid – it merely provides a lower bound [40, 41]. Band & Boyland [42] showed the Burau eigenvalue gives the exact topological entropy for a pseudo-Anosov braid if and only if the corresponding foliation has odd-order singularities at all the punctures, and any interior singularities are of even order. One consequence is that the Burau bound is always sharp for 3-braids, a fact we used in Section 2.1 to compute the entropy.

Figure 4 shows material line patterns for some four-rod mixers. Table 2 lists the braid, the measured topological entropy ( $h$ ), the topological entropy of the braid ( $h_{\text{rods}}$ ) given by the Bestvina–Handel algorithm [43, 44], the Burau bound, the sign of the dominant eigenvalue in the Burau matrix, and size of the gap between the two topological entropy values. Observe that again the braids with a positive Burau eigenvalue have small gaps in entropy – less

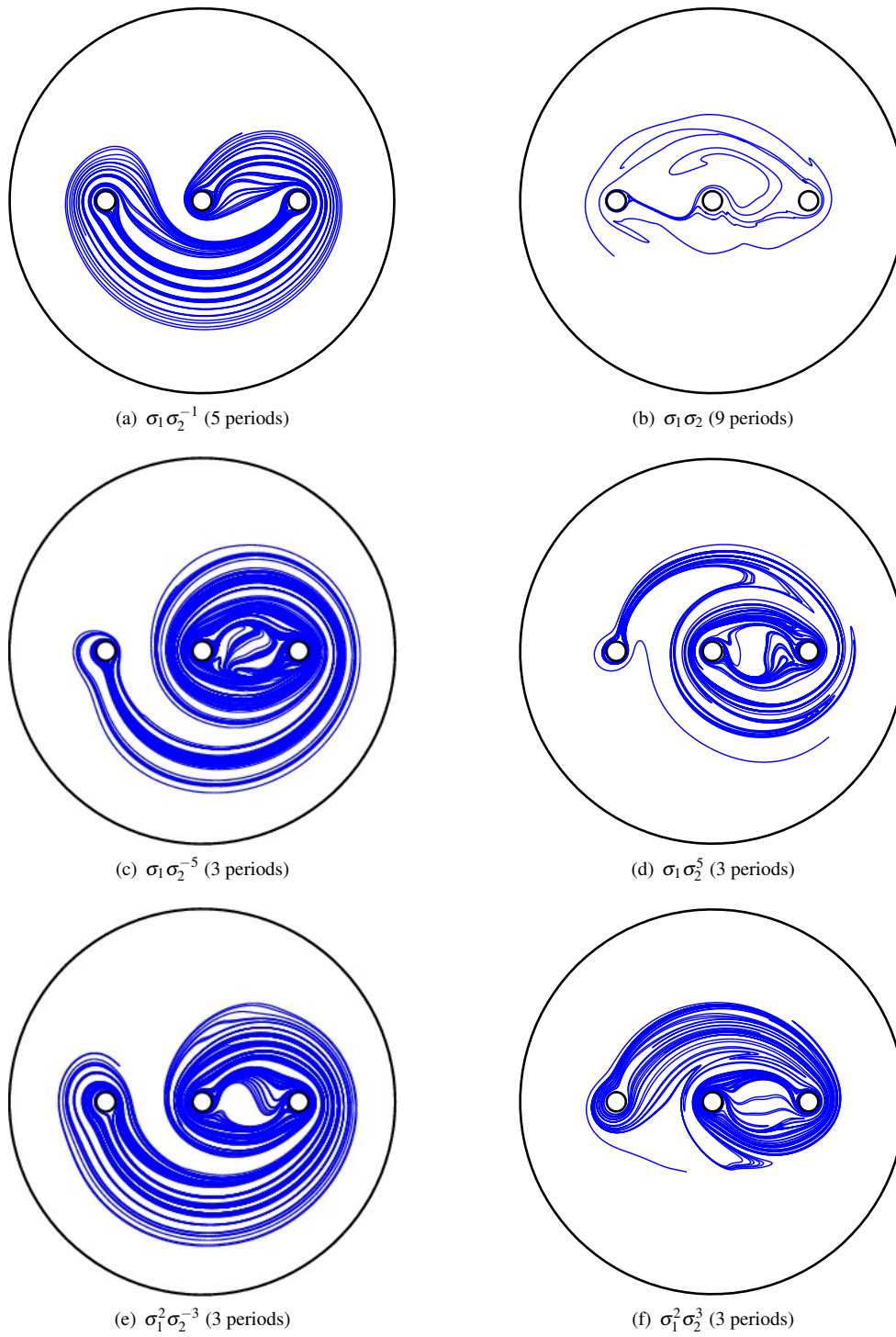


Fig. 2. Material line patterns for several three-rod braid mixers.

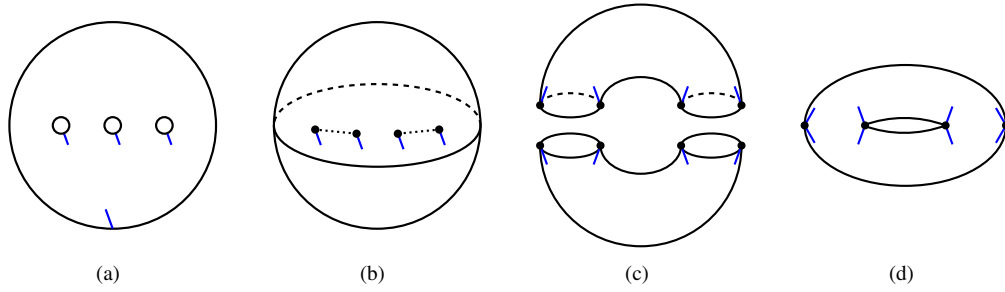


Fig. 3. How to make the orientation double cover. (a) A disk with three rods, the small segments indicating pronged singularities. (b) Shrink the disk's boundary and the rods to points, so the surface is a topological sphere. Make two cuts between the rods and the boundary (dotted lines). (c) Glue a second copy of the same sphere along the cuts. (d) The resulting surface is a torus, and the singularities now have two prongs (regular points).

Table 1. Measured topological entropy vs. the lower bound for 3-rod braid mixers. The sign listed is that of the dominant eigenvalue in the Burau matrix.

braid	$h$	$h_{\text{rods}}$	Burau sign	gap
$\sigma_1 \sigma_2^{-1}$	0.992	0.9624	pos	3.0%
$\sigma_1 \sigma_2^{-2}$	1.380	1.3170	pos	4.6%
$\sigma_1 \sigma_2^{-3}$	1.714	1.5668	pos	8.6%
$\sigma_1 \sigma_2^{-4}$	2.048	1.7627	pos	13.9%
$\sigma_1 \sigma_2^{-5}$	2.112	1.9248	pos	8.9%
$\sigma_1^2 \sigma_2^{-2}$	1.867	1.7627	pos	5.6%
$\sigma_1^2 \sigma_2^{-3}$	2.244	2.0634	pos	8.0%
$\sigma_1^2 \sigma_2^{-4}$	2.612	2.2924	pos	12.2%
$\sigma_1 \sigma_2$	0.289	0		100%
$\sigma_1 \sigma_2^2$	0.550	0		100%
$\sigma_1 \sigma_2^3$	1.109	0		100%
$\sigma_1 \sigma_2^4$	1.829	0		100%
$\sigma_1 \sigma_2^5$	1.611	0.9624	neg	40.3%
$\sigma_1^2 \sigma_2^2$	1.328	0		100%
$\sigma_1^2 \sigma_2^3$	1.762	1.3170	neg	25.3%
$\sigma_1^2 \sigma_2^4$	2.455	1.7627	neg	28.2%

than 2%. We will discuss the sources of discrepancy in the next section.

### 3. Explaining the gap

Our ultimate goal is to predict when the lower bound from the rod motion is close to the measured topological entropy (small gap), and when it is not (large gap). Furthermore, we wish to understand what causes a large gap, that is: what is it about the flow that creates more topological entropy? The easier question to answer, at least partially, is why the lower bound fails. We will address this first. Then we will attempt to explain why it happens.

#### 3.1. Why there is a gap – secondary folding

Recall that the lower bound on entropy arises from the braid giving the rod motion: this braid labels the isotopy class of the period-1 map. Since the pseudo-Anosov representative of the isotopy class is the ‘simplest’ map in the class (the one with the lowest entropy), the isotopy from the flow to the pseudo-Anosov representative has the effect of pulling tight the material lines. In order for the flow to have a higher topological entropy, there must be some part of the material line pattern that is not already pulled-tight. In other words, there must be some extra folding that is not directly due to the rods. We call this *secondary folding* [28, 29]. Figure 5(a) shows an example of folding due to a rod, and Figure 5(b) shows secondary folding, which is not associated with a rod and could be removed by pulling

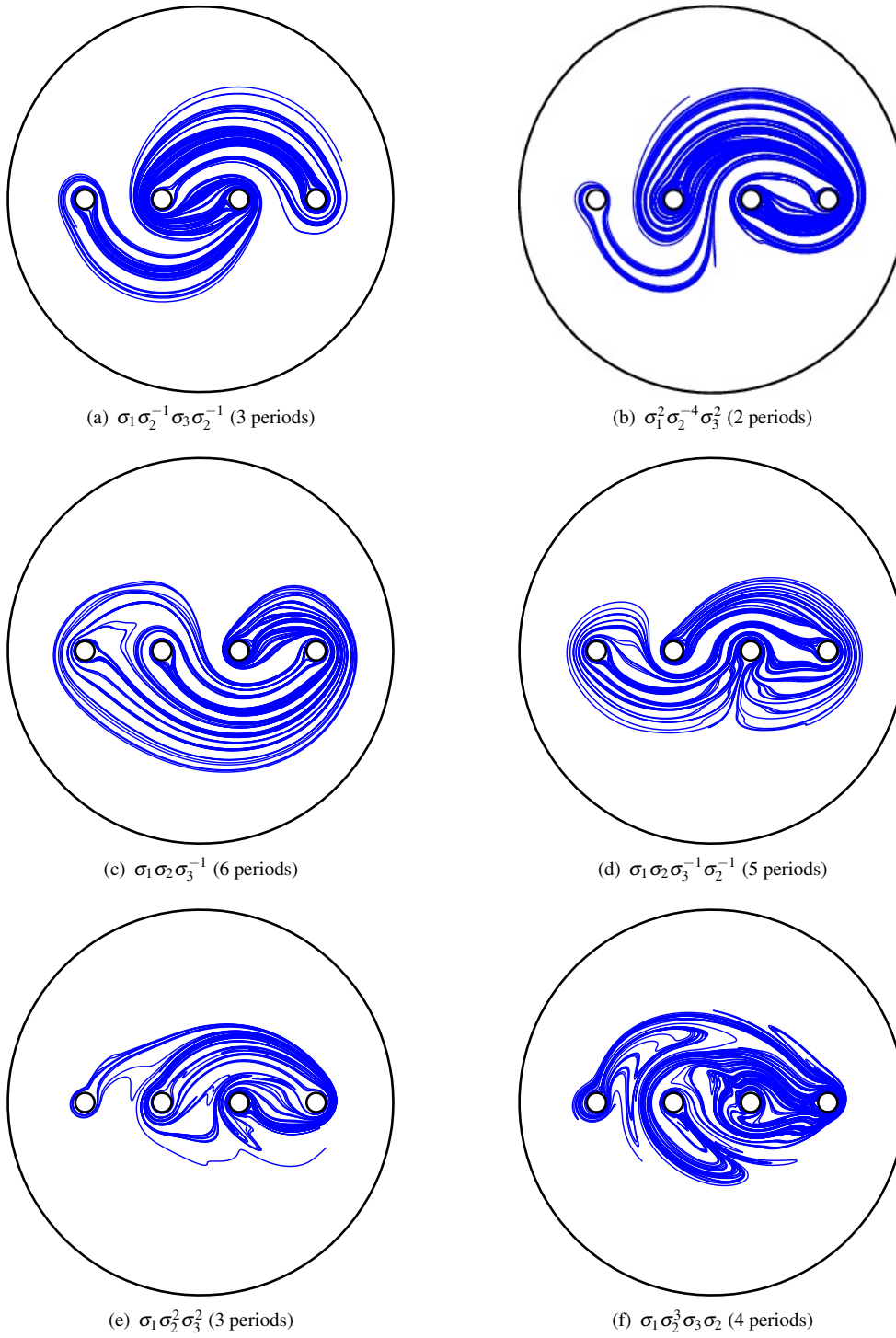


Fig. 4. Material line patterns for several four-rod braid mixers.

Table 2. Measured topological entropy vs. the lower bounds for 4-rod braid mixers. The sign listed is that of the dominant eigenvalue in the Burau matrix. The braids in the last set have vanishing Burau bound, so no sign is ascribed, except for the last braid (marked with  $^\dagger$ ) where we found the action on homology to be positive (Section 4).

braid	$h$	$h_{\text{rods}}$	Burau bound	Burau sign	gap
$\sigma_1 \sigma_2^{-1} \sigma_3 \sigma_2^{-1}$	1.949	1.92485	1.92485	pos	1.2%
$\sigma_1 \sigma_2 \sigma_3^{-1} \sigma_2^{-1}$	0.970	0.96242	0.96242	pos	0.8%
$\sigma_1 \sigma_3 \sigma_2^{-1}$	1.319	1.31696	1.31696	pos	0.2%
$\sigma_1^2 \sigma_2^{-2} \sigma_3^2 \sigma_2^{-2}$	3.559	3.52549	3.52549	pos	0.9%
$\sigma_1^2 \sigma_2^{-4} \sigma_3^2$	2.940	2.88727	2.88727	pos	1.8%
$\sigma_1^2 \sigma_2^{-2} \sigma_3^2$	2.303	2.29243	2.29243	pos	0.5%
$\sigma_1 \sigma_2^2 \sigma_3^2$	1.562	1.31696	1.31696	neg	15.7%
$\sigma_1^2 \sigma_2^{-1} \sigma_3 \sigma_2^2$	1.914	1.56686	1.56686	neg	18.1%
$\sigma_1 \sigma_2^2 \sigma_3 \sigma_2$	1.270	0.96242	0.96242	neg	24.2%
$\sigma_1^2 \sigma_3^2 \sigma_2^2$	1.903	1.76275	1.76275	neg	7.4%
$\sigma_1 \sigma_2 \sigma_3 \sigma_2$	0.509	0	0		100%
$\sigma_1 \sigma_2^{-1} \sigma_3^{-1} \sigma_2^{-1}$	1.065	0.96242	0		9.6%
$\sigma_1 \sigma_3 \sigma_2$	0.275	0	0		100%
$\sigma_1 \sigma_2 \sigma_3^{-1}$	0.837	0.83144	0	pos $^\dagger$	0.7%

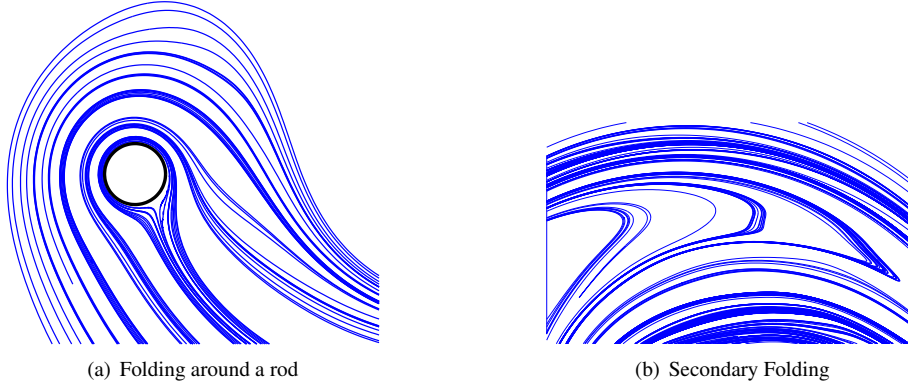


Fig. 5. (a) Folding caused by a rod moving through the fluid and dragging along the material lines. (b) Secondary folding of the material line. This is not directly associated with folding around a rod and can be ‘pulled tight’ via homotopy.

tight.

Having a few extra folds is not necessarily enough to cause higher topological entropy. Recall that for 2D systems topological entropy is related to the exponential stretching rate of material lines [36, 37, 38]. The extra folds must cause a higher line growth rate in order to affect the topological entropy.

Looking back at the three-braid mixers shown in Figure 2, there is visible secondary folding in the  $\sigma_1 \sigma_2^5$  and  $\sigma_1^2 \sigma_2^3$  mixers. From Table 1, we see that these had gaps of 40.3% and 25.3% respectively. In contrast, the  $\sigma_1 \sigma_2^{-1}$ ,  $\sigma_1 \sigma_2^{-5}$ , and  $\sigma_1^2 \sigma_2^{-3}$  mixers have no visible secondary folding, and have gaps of 3.0%, 8.9%, and 8.0% respectively. The same can be seen in the four-rod braid mixers of Figure 4. There is visible secondary folding in the  $\sigma_1 \sigma_2^2 \sigma_3^2$  and  $\sigma_1 \sigma_2^3 \sigma_3 \sigma_2$  mixers, and these have gaps of 15.7% and 24.2% respectively. In comparison, for the  $\sigma_1 \sigma_2^{-1} \sigma_3 \sigma_2^{-1}$ ,  $\sigma_1^2 \sigma_2^{-4} \sigma_3^2$ ,  $\sigma_1 \sigma_2 \sigma_3^{-1}$ , and  $\sigma_1 \sigma_2 \sigma_3^{-1} \sigma_2^{-1}$  mixers there is no visible secondary folding, with gaps of 1.2%, 1.8%, 0.7%, and 0.8% respectively.

### 3.2. When there is a gap – negative eigenvalues

We would now like to predict *when* we can expect a gap between the measured topological entropy and the lower bound given by the braid. From the data presented, it is tempting to say that mixers with a braid whose Burau matrix has a negative dominant eigenvalue have a large gap, while those with positive eigenvalues have a small gap. However,

this says nothing about braids for which the Burau bound is zero. Furthermore, the data does not include any braids whose Burau bound is non-zero, but also not equal to the topological entropy of the braid (because of odd interior singularities in the foliation). We discuss why we didn't include such braids in Section 4. However, it is clear at this point that the sharpness is closely correlated with the sign of the action on first homology of the orientation double cover, as given by the Burau representation in most cases examined here.

#### 4. Discussion

In summary, we have exhibited a number of examples of braid-based rod mixers. These fall in two categories: those for which the rod motion is a good predictor of the flow entropy, and those for which it isn't. For both three- and four-rod systems, the sign of the Burau eigenvalue correlates well with the two cases: a positive eigenvalue usually means that the bound is sharp.

When the Burau entropy is not sharp, the relevant quantity is the sign of the action of the braid on homology lifted to the orientation double cover. When the sign is negative, then the entire homological chain must 'flip' which each action of the braid. The conjecture is that this flip causes secondary folding by promoting 'slack' in the material lines. This is evident when examining toral linked twist maps [28, 29]. Unfortunately, this cannot be the whole story, since repeating the rod motion twice will always make the homological eigenvalue positive, but will clearly not make the lower bound any better.

Why is the orientation double cover important? The foliations obtained on disks are always non-orientable, due to the odd-pronged singularities at the rods. The orientation double cover turns the disk foliation into an orientable foliation on a closed surface of some genus (a torus in Figure 3). It is then easy to compute the topological entropy, since the linear action on homology gives the entropy for the case of orientable foliations. However, in order to construct the orientation double cover we need to know *a priori* the odd-pronged singularities associated with a braid's isotopy class.

In general we should be able to ascribe a homological sign even for braids that are not Burau-sharp. This is easy to do when a pseudo-Anosov is given in terms of Dehn twists on the double cover [45], but is not so straightforward when starting from braids on the disk; this is a future challenge. For the braid  $\sigma_1 \sigma_2 \sigma_3^{-1}$  in Table 2, we were able to determine that the sign is positive by puncturing at the 3-pronged singularity and computing the Burau action of the resulting 5-braid  $((\sigma_1 \sigma_2 \sigma_1) \sigma_3 \sigma_4^{-1})$ . Note that both homological signs can always be realised, since the braids giving rise to different signs are related by the deck transformation (involution) of the double cover [46].

#### Acknowledgements

The authors thank Phil Boyland for his patient help. J-LT is grateful for the hospitality of the Isaac Newton Institute for Mathematical Sciences in Cambridge, UK. This work was funded by the Division of Mathematical Sciences of the US National Science Foundation, under grant DMS-0806821.

#### References

- [1] Boyland PL, Aref H, Stremler MA. Topological fluid mechanics of stirring. *J Fluid Mech.* 2000;403:277–304.
- [2] Finn MD, Cox SM, Byrne HM. Topological chaos in inviscid and viscous mixers. *J Fluid Mech.* 2003;493:345–361.
- [3] Vkhansky A. Simulation of Topological Chaos in Laminar Flows. *Chaos.* 2004 Mar;14(1):14–22.
- [4] Finn MD, Thiffeault JL, Gouillart E. Topological Chaos in Spatially Periodic Mixers. *Physica D.* 2006 Sep;221(1):92–100.
- [5] Finn MD, Thiffeault JL. Topological Entropy of Braids on the Torus. *SIAM J Appl Dyn Sys.* 2007;6:79–98.



- [6] Kobayashi T, Umeda S. Realizing pseudo-Anosov egg beaters with simple mechanisms. In: Proceedings of the International Workshop on Knot Theory for Scientific Objects, Osaka, Japan. Osaka Municipal Universities Press; 2007. p. 97–109.
- [7] Binder BJ, Cox SM. A Mixer Design for the Pigtail Braid. *Fluid Dyn Res.* 2008;40:34–44.
- [8] Thiffeault JL, Finn MD, Gouillart E, Hall T. Topology of Chaotic Mixing Patterns. *Chaos.* 2008 Sep;18:033123.
- [9] Boyland PL, Harrington J. The entropy efficiency of point-push mapping classes on the punctured disk. *Algeb Geom Topology.* 2011;11(4):2265–2296.
- [10] Finn MD, Thiffeault JL. Topological optimisation of rod-stirring devices. *SIAM Rev.* 2011 Dec;53(4):723–743.
- [11] Boyland PL, Stremler MA, Aref H. Topological fluid mechanics of point vortex motions. *Physica D.* 2003;175:69–95.
- [12] Boyland PL. Dynamics of two-dimensional time-periodic Euler fluid flows. *Topology Appl.* 2005;152:87–106.
- [13] Gouillart E, Finn MD, Thiffeault JL. Topological Mixing with Ghost Rods. *Phys Rev E.* 2006;73:036311.
- [14] Stremler MA, Chen J. Generating topological chaos in lid-driven cavity flow. *Phys Fluids.* 2007;19:103602.
- [15] Thiffeault JL, Gouillart E, Finn MD. The Size of Ghost Rods. In: Cortelezzi L, Mezić I, editors. *Analysis and Control of Mixing with Applications to Micro and Macro Flow Processes.* vol. 510 of CISM International Centre for Mechanical Sciences. Vienna: Springer; 2009. p. 339–350.
- [16] Binder BJ. Ghost rods adopting the role of withdrawn baffles in batch mixer designs. *Phys Lett A.* 2010;374:3483–3486.
- [17] Stremler MA, Ross SD, Grover P, Kumar P. Topological Chaos and Periodic Braiding of Almost-Cyclic Sets. *Phys Rev Lett.* 2011;106:114101.
- [18] Vikhansky A. Chaotic advection of finite-size bodies in a cavity flow. *Phys Fluids.* 2003 Jul;15(7):1830–1836.
- [19] Kin E, Sakajo T. Efficient topological chaos embedded in the blinking vortex system. *Chaos.* 2005;15(2):023111.
- [20] Thiffeault JL. Measuring Topological Chaos. *Phys Rev Lett.* 2005 Mar;94(8):084502.
- [21] Allshouse MR, Thiffeault JL. Detecting coherent structures using braids. *Physica D.* 2012 Jan;241(2):95–105.
- [22] Thiffeault JL. Braids of entangled particle trajectories. *Chaos.* 2010 Jan;20:017516.
- [23] Turner MR, Berger MA. A study of mixing in coherent vortices using braiding factors. *Fluid Dyn Res.* 2011 Jun;43(3):035501.
- [24] Puckett JG, Lechenault F, Daniels KE, Thiffeault JL. Trajectory entanglement in dense granular materials. *Journal of Statistical Mechanics: Theory and Experiment.* 2012 Jun;2012(6):P06008. Available from: <http://iopscience.iop.org/1742-5468/2012/06/P06008>.
- [25] Finn MD, Cox SM, Byrne HM. Chaotic advection in a braided pipe mixer. *Phys Fluids.* 2003 Nov;15(11):L77–L80.
- [26] Thiffeault JL, Finn MD. Topology, Braids, and Mixing in Fluids. *Phil Trans R Soc Lond A.* 2006 Dec;364:3251–3266.
- [27] Thiffeault JL, Lanneau E, Matz SE. The cat's cradle, stirring, and topological complexity; 2009. <http://www.dynamicalsystems.org/ma/ma/display?item=292>. *Dynamical Systems Magazine.*
- [28] Tumas SE, Thiffeault JL. Topological entropy and secondary folding; 2012. <http://arXiv.org/abs/1204.6730>.

- [29] Tumaş SE. Topological Stirring. University of Wisconsin – Madison. Madison, WI; 2012.
- [30] Artin E. Theory of Braids. *Ann Math.* 1947 Jan;48(1):101–126.
- [31] Birman JS. Braids, Links, and Mapping Class Groups. No. 82 in *Annals of Mathematics Studies*. Princeton, NJ: Princeton University Press; 1975.
- [32] Birman JS, Brendle TE. Braids: A Survey. In: Menasco W, Thistlethwaite M, editors. *Handbook of Knot Theory*. Amsterdam: Elsevier; 2005. p. 19–104. Available at <http://arXiv.org/abs/math.GT/0409205>.
- [33] Fathi A, Laudenbach F, Poénaru V. *Travaux de Thurston sur les surfaces*. *Astérisque*. 1979;66-67:1–284.
- [34] Thurston WP. On the geometry and dynamics of diffeomorphisms of surfaces. *Bull Am Math Soc.* 1988;19:417–431.
- [35] Boyland PL. Topological methods in surface dynamics. *Topology Appl.* 1994;58:223–298.
- [36] Yomdin Y. Volume growth and entropy. *Israel J Math.* 1987;57(3):285–300.
- [37] Newhouse SE. Entropy and volume. *Ergod Th Dynam Sys.* 1988;8:283–299.
- [38] Newhouse SE, Pignataro T. On the estimation of topological entropy. *J Stat Phys.* 1993;72(5-6):1331–1351.
- [39] Burau W. Über Zopfgruppen und gleichsinnig verdrehte Verkettungen. *Abh Math Semin Hamburg Univ.* 1936;11:171–178.
- [40] Fried D. Entropy and twisted cohomology. *Topology.* 1986;25(4):455–470.
- [41] Kolev B. Entropie topologique et représentation de Burau. *C R Acad Sci Sér I.* 1989;309(13):835–838. English translation at <http://arxiv.org/abs/math.DS/0304105>.
- [42] Band G, Boyland PL. The Burau estimate for the entropy of a braid. *Algeb Geom Topology.* 2007;7:1345–1378.
- [43] Bestvina M, Handel M. Train-Tracks for Surface Homeomorphisms. *Topology.* 1995;34(1):109–140.
- [44] Hall T. *Train: A C++ program for computing train tracks of surface homeomorphisms*. [http://www.liv.ac.uk/math/PURE/MIN\\_SET/CONTENT/members/T.Hall.html](http://www.liv.ac.uk/math/PURE/MIN_SET/CONTENT/members/T.Hall.html).
- [45] Lanneau E, Thiffeault JL. On the minimum dilatation of pseudo-Anosov homeomorphisms on surfaces of small genus. *Ann Inst Fourier.* 2011;61(1):105–144.
- [46] Lanneau E, Thiffeault JL. On the minimum dilatation of braids on the punctured disc. *Geometriae Dedicata.* 2011 Jun;152(1):165–182.